Published in IET Microwaves, Antennas & Propagation
Received on 17th December 2008
Revised on 31st July 2009
doi: 10.1049/iet-map.2009.0084

ISSN 1751-8725

Pure left-handed transmission line

Y.-H. Ryu[1] *J.-H. Park*[2] *J.-H. Lee*[2] *H.-S. Tae*[1]

[1]*School of Electrical Engineering and Computer Science, Kyungpook National University, Daegu 702-701, Korea*
[2]*School of Electronic and Electrical Engineering, Hongik University, Seoul 121-791, Korea*
E-mail: jeonglee@hongik.ac.kr

Abstract: The pure left-handed transmission line (PLH TL) for a broad left-handed (LH) band is presented. It consists of a defected ground structure (DGS) and a wire bonded inter-digital capacitor (WBIDC). The bridged connection of vias to ground makes the components of inductance and capacitance effectively negative. These negative components exclude a parasitic right-handed branch so that the transmission line has only a pure left-handed branch. The equivalent circuit of a bridge type is provided to analyse the structure. The dispersion and *S*-parameter characteristics of the PLH TL are analysed by circuit analysis, Bloch–Floquet theory, and full-wave simulation. The measured results of dispersion curves and frequency behaviours have good agreements with those of theory and simulation. An optimised PLH TL with wide LH fractional bandwidth of 140% is also designed.

1 Introduction

Over the past decade, various metamaterials with exotic material constants have evolved with novel electromagnetic concepts such as backward wave propagation, negative index refraction and infinite wavelength wave propagation [1, 2]. In particular, planar meta-structured transmission lines (MTLs) are broadly applied to various radio frequency (RF) devices such as filters, couplers, antennas, resonators, power dividers and baluns because of low loss, convenience of theoretical analysis and simplicity of the fabrication [3]. However, most of MTLs have a spurious right-handed (RH) branch because of an inherent series inductance and shunt capacitance, resulting in a limited left-handed (LH) band [4–6]. If a spurious RH branch were removed, a broader LH band would be obtained. This pure left-handed transmission line (PLH TL) could be easily applied to a wide band RF application.

The main purposes of this paper are to implement the PLH TL using distributed structures, to design the PLH TL with a broad LH bandwidth and to show the design flexibility of the PLH TL. A PLH TL without RH band is first realised using a defected ground structure (DGS) with a wire bonded inter-digital capacitor (WBIDC). The cross connection of vias gives rise to the negative values of inductance and capacitance. These negative components can make the effective negative epsilon in the reduced Brillouin zone (BZ) [7]. It is noted that the reduced BZ is defined by $0 < \beta d < \pi$, where βd of π corresponds to half a guided wavelength on one-dimensional (1-D) structure. The PLH TL has no RH branch which would appear in the dispersion curves of conventional MTLs. Thus, the PLH TL only has a LH band in the BZ. To achieve the broad PLH band and remove the spurious modes that are a major drawback of inter-digital capacitor (IDC) [8, 9], a WBIDC is employed. Using circuit analysis, full-wave simulation and measurement, the properties of the PLH TL will be analysed. To design a PLH TL with a wide LH bandwidth, parameter studies are performed using an equivalent circuit.

2 Structure and exact equivalent circuit of proposed PLH TL

Fig. 1 shows the proposed PLH TL structure. The unit cell consists of a DGS with WBIDC, vias and a conventional microstrip signal line. In Fig. 1*b*, to broaden the LH band and remove spurious modes of an IDC, a WBIDC is employed because the IDC, a multi-conductor structure, has spurious modes in relatively lower frequency range [8, 9]. To realise the PLH TL, the position of via is very important in design of the unit cell. It is a key point that the signal line is connected to the end of each finger of the WBIDC in the ground plane by vias as shown in Fig. 1. That is, in Fig. 1*a*, the via near port 1 of the signal line is

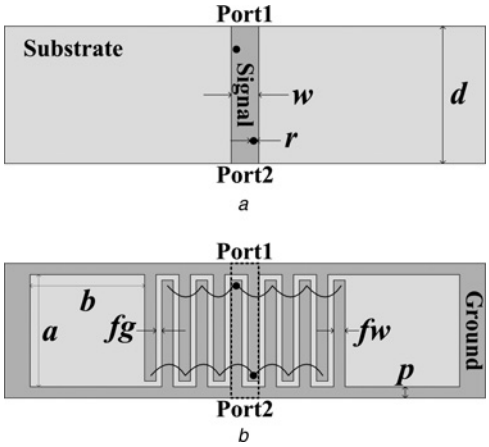

Figure 1 *Structure of PLH TL*

a Top view
b Bottom view
($a = b = 5$ mm, $w = 1.1$ mm, $fg = 0.1$ mm, $fw = 0.5$ mm, $r = 0.3$ mm, $p = 0.1$ mm, the number of finger pairs = 6, unit cell length (d) = 5.2 mm)

connected to the ground plane which links to port 2 in Fig. 1*b* and vice versa.

Consequently, from a viewpoint of signal flow, the circuit model of a unit cell is exactly represented by a 4-(or balanced) terminal network with cross-connected circuit as shown in Fig. 2*a*. Fig. 2 shows the equivalent circuits of the unit cell of the proposed PLH TL. A WBIDC overcomes the drawback of the IDC by interconnecting the ends of the fingers. That is, the WBIDC, which has almost the same value of capacitance with that of the IDC, operates as a capacitor over the wide range of frequency since these bonding wires prevent the spurious modes of the IDC [8]. Also, the DGS is realised by etching a defected pattern on the ground plane of 1-D TLs as shown in Fig. 1*b*. The DGS is equivalently modelled as a parallel resonant circuit as shown in Fig. 2*a* [10]. In Fig. 2, the capacitance (C_d) and inductance (L_d) of the parallel resonance circuit because of DGS depend on the number of inter-digital fingers and/or their gap width and the etched rectangular size, respectively. The inductance (L_{t1}) is determined by the length of the signal line between vias. Also, the capacitance (C_t) and inductance (L_t) of the host TL are parasitic elements of the proposed PLH TL.

To explain how to obtain the negative value of L and C in Fig. 1*b*, the cross-connected part of the original circuit model in Fig. 2*a* is simply represented as the circuit in Fig. 2*c* constituted by Z_1 and Z_2. Then, the cross-connected circuit can be changed directly to the bridged circuit as shown in Fig. 2*d* by the rearrangement of the circuit. The bridged circuit can be converted directly to π-equivalent circuit with the reversed direction of V_2 and I_2 at port 2 as shown in Fig. 2*e*. Therefore the cross-connected part in Fig. 2*a* can be converted directly to T-equivalent circuit with impedance (Z) and admittance (Y) and common ground as shown in Fig. 2*b* using r-parameters [11]. The r-parameters are expressed as follows

$$r_{11} = r_{22} = \frac{-\omega^2 L_{t1} L_d}{j\omega(L_{t1} + L_d - \omega^2 C_d L_{t1} L_d)} = Z_1 \parallel Z_2 \quad (1a)$$

$$r_{12} = r_{21} = \frac{\omega^2 L_{t1} L_d}{j\omega(L_{t1} + L_d - \omega^2 C_d L_{t1} L_d)} = -Z_1 \parallel Z_2 \quad (1b)$$

where $Z_1 = j\omega L_{t1}$ and

$$Z_2 = \frac{j\omega L_d}{1 - \omega^2 C_d L_d} \quad (2)$$

Here, r_{12} (r_{21}) is obtained by relation of V_1 and I_2 when the port 1 is open ($I_1 = 0$). In this case, the direction of the current of I_2 is opposite to the voltage of V_1 as shown in Fig. 2*d*. Therefore the resulting impedance is represented by parallel value of Z_1 and Z_2 with negative sign as (1b). Therefore the impedance (Z) and admittance (Y) are expressed as the following

$$Z = r_{11} - r_{12} = r_{22} - r_{21} = 2 \times \frac{Z_1 Z_2}{Z_1 + Z_2} = \frac{2\omega^2 L_{t1} L_d}{j\omega(\omega^2 C_d L_{t1} L_d - L_{t1} - L_d)} \quad (3a)$$

$$Y = 1/r_{12} = -\frac{Z_1 + Z_2}{Z_1 Z_2} = -\frac{j\omega(\omega^2 C_d L_{t1} L_d - L_{t1} - L_d)}{\omega^2 L_{t1} L_d} = \frac{j\omega(\omega^2(-C_d)(-L_{t1})(-L_d) - (-L_{t1}) - (-L_d))}{\omega^2(-L_{t1})(-L_d)} \quad (3b)$$

It is noted that the negative value of admittance results from the reversed current direction, which is due to the cross connection of the structure, with respect to the voltage. From (3b), it is also known that the admittance value (Y) has the most important information. That is, the admittance value (Y) corresponding to effective epsilon has the negative values of parallel composition of Z_1 and Z_2. To have the parallel composition of Z_1 and Z_2 to be the negative value, there is only one choice that all elements of the admittance must have negative values in (3b). Consequently, the modified equivalent circuit with common ground can be represented as Fig. 2*b*. Also, the modified equivalent circuit can be reduced to simple T-equivalent circuit by successive applications of T–Π transformations [11] as shown in Fig. 2*f*. Thus, a total impedance and admittance are as follows

$$Z_T = 2Z_t \quad \text{and} \quad Y_T = Y_t \quad (4)$$

Then, the effective permeability and permittivity values are obtained from $\mu_{eff} = Z_T(\omega)/j\omega d$ and $\varepsilon_{eff} = Y_T(\omega)/j\omega d$ [1]. By applying the periodic boundary condition related with Bloch–Floquet theorem to the equivalent circuit, the

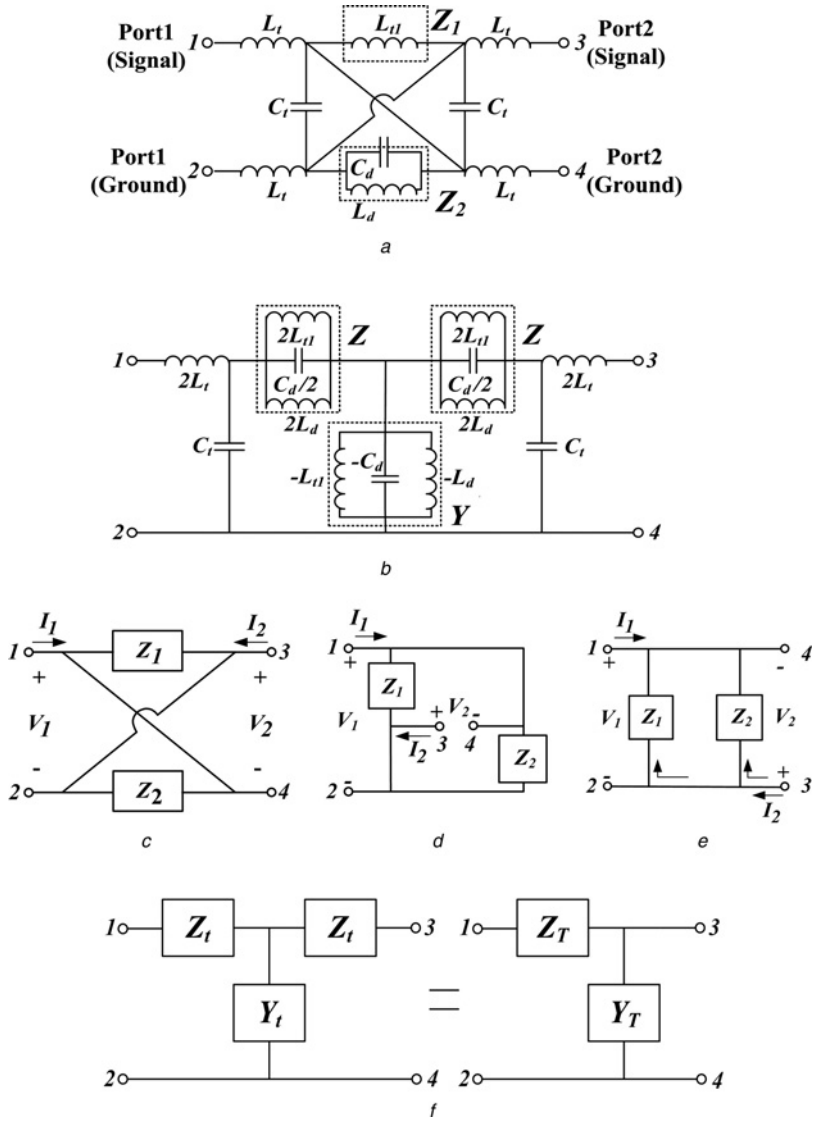

Figure 2 *Equivalent circuits*

a Original four-terminal network
b Modified three-terminal network with common ground
c Cross-connected part
d Bridged circuit
e π-Equivalent circuit with the reverse direction of V_2 and I_2
f T and ladder-equivalent circuit of the unit cell

propagation constant (γ) is represented as follows [12]

$$\gamma(\omega) = a(\omega) + j\beta(\omega) \tag{5}$$

where $\alpha(\omega) = 1/d \cosh^{-1}[1 + (Z_T Y_T/2)]$ and $\beta(\omega) = 1/d \cos^{-1}[1 + (Z_T Y_T/2)]$.

The α and β are attenuation and phase constants for Bloch waves and d is the periodicity of the structure. The circuit parameters of Figs. 2*a* and *b* can be extracted by circuit simulation (Ansoft's Designer) and full-wave simulation (Ansoft's HFSS). The extracted circuit parameters are $L_d = 4.57$ nH, $C_d = 8.20$ pF, $C_t = 0.24$ pF, $L_t = 0.28$ nH and $L_{t1} = 1.36$ nH, respectively.

It is important to note that the negative elements such as $-C_d$, $-L_{t1}$ and $-L_d$ in Fig. 2*b* appear in the modified equivalent circuit. These negative elements can be induced from the cross-connected circuit as shown in Fig. 2*a*. Owing to these negative elements, the imaginary part of Y_T corresponding to an effective epsilon monotonically decreases with negative sign as the frequency increases, as will be shown in Fig. 3*a*. Consequently, there is no RH band and the PLH TL over a whole frequency can be theoretically realised.

To intuitively expect the properties of a PLH TL and give a design guideline of a PLH TL, a parameter study of a PLH TL has been executed by the equivalent circuit and circuit simulator. The role of the RH elements of the PLH TL is

IET Microw. Antennas Propag., 2010, Vol. 4, Iss. 6, pp. 792–798

doi: 10.1049/iet-map.2009.0084

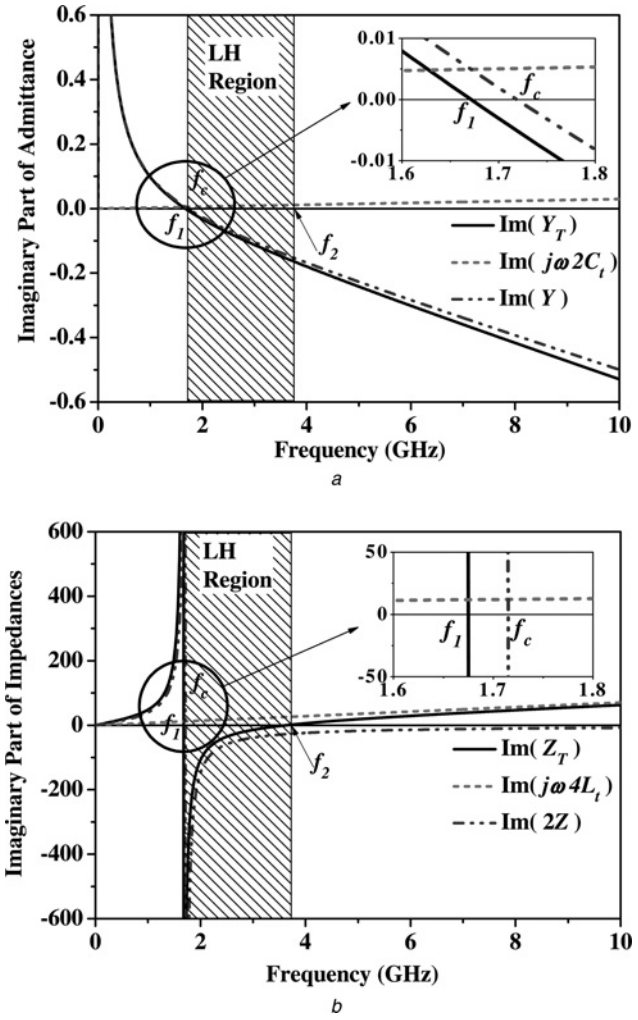

Figure 3 *Imaginary parts*

a Admittance
b Impedance
(Circuit simulation result using Ansoft's Designer)

investigated in detail. In the equivalent circuit of Fig. 2, the RH elements of the host TL are C_t, L_t and L_{t1} as parasitic elements whereas the cross connection of vias between the signal line and ground and the elements of C_d and L_d are to realise a PLH TL.

Fig. 3 shows the imaginary parts of admittance and impedance, corresponding to ε_{eff} and μ_{eff}, respectively. In Fig. 3, the values of $\mathrm{Im}(Z_T, Y_T)$, $\mathrm{Im}(2Z, Y)$ and $\mathrm{Im}(j\omega 4L_t, j\omega 2C_t)$ of Fig. 2 are compared. Although the exact values of $\mathrm{Im}(Y_T)$ and $\mathrm{Im}(Z_T)$ are obtained by successive calculation using T–Π transformations, the ε_{eff} and μ_{eff} can be obtained approximately as follows

$$\varepsilon_{eff} = \frac{\mathrm{Im}(Y_T)/d}{\omega} \simeq \frac{\mathrm{Im}(Y)/d}{\omega} \quad \text{and}$$
$$\mu_{eff} = \frac{\mathrm{Im}(Z_T)/d}{\omega} \simeq \frac{\mathrm{Im}(j\omega 4L_t + 2Z)/d}{\omega} \tag{6}$$

The reason for the above approximation is that the value of $\mathrm{Im}(Y)$ is much larger than that of ωC_t and, thus, the extremely small value of ωC_t is operated as an open circuit. Fig. 3*a* shows that the $\mathrm{Im}(Y_T)$ corresponding to an ε_{eff} monotonically decreases with negative sign as the frequency increases above cutoff frequency of f_1 (1.67 GHz) whereas that of a CRLH TL increases [1–3] as the frequency increases. Thus, the TL cannot have the effectively positive ε above the cutoff frequency of f_1 because of the negative elements of $-C_d$, $-L_{t1}$, and $-L_d$. Fig. 3*b* shows the $\mathrm{Im}(Z_T)$ corresponding to a μ_{eff}. The $\mathrm{Im}(Z_T)$ is approximately obtained by superposition of $\mathrm{Im}(2Z)$ and $\mathrm{Im}(j\omega 4L_t)$ as shown in Fig. 3*b*. It is directly known that L_t determines the cutoff frequency of f_2. That is, the range of the negative μ is determined by L_t in BZ. Consequently, the LH band is from f_1 to f_2 without RH band in BZ because the effective ε monotonically decreases with negative sign. In addition, these RH parasitic elements of C_t and L_t shift lower frequency cutoff of f_c (1.72 GHz) to f_1 (1.67 GHz) as shown in Fig. 3. The component of L_{t1} affects the cutoff frequencies of f_1 and f_2 in Fig. 3. As the component of L_{t1} increases, the cutoff frequencies of f_1 and f_2 downshift whereas the frequency range between f_1 and f_2 increases. It leads to broaden the LH bandwidth. Consequently, the components of L_t and L_{t1} determine the LH band and the component of C_t has little effect on the LH band.

The cutoff frequency of f_c is easily calculated by the condition of $Y = 0$ (or $Z = \infty$) and is given as

$$\omega_c = \sqrt{\frac{L_{t1} + L_d}{C_d L_d L_{t1}}} \tag{7}$$

Also, it is noted that the cutoff frequencies of f_1 and f_2 are easily calculated by (5) with condition of $\beta = 0$ or π. Below the cutoff frequency of f_1, the absolute values of $1 + Z_T Y_T/2$ are larger than one. Thus, in the region, the propagation constant of γ has only attenuation constant of α. Then, a wave does not propagate but is attenuated along the line. Therefore this region is corresponding to a rejection band [13], although the material constants have both positive values. Above the high frequency cutoff of f_2, it is a rejection band since the effective permeability is positive and the effective permittivity is negative.

To be compared with a LH bandwidth of CRLH TL, the LH bandwidth of a PLH TL is calculated by varying the values of the circuit elements (L_{t1}, C_t, L_t). Fig. 4 shows the calculated fractional LH bandwidth when only one value of the component increases from 0.1 to 10 (pF or nH) with the other components fixed. As an example, the solid line is the calculated fractional LH bandwidth where the value of L_{t1} increases from 0.1 to 10 nH and the other components are fixed ($L_d = 4.57$ nH, $C_d = 8.20$ pF, $C_t = 0.24$ pF, $L_t = 0.28$ nH). In Fig. 4, it is found that the fractional LH bandwidth increases in proportion to the inductance values of L_{t1} and in inverse proportion to the inductance value of L_t. It is also shown that the fractional bandwidth is

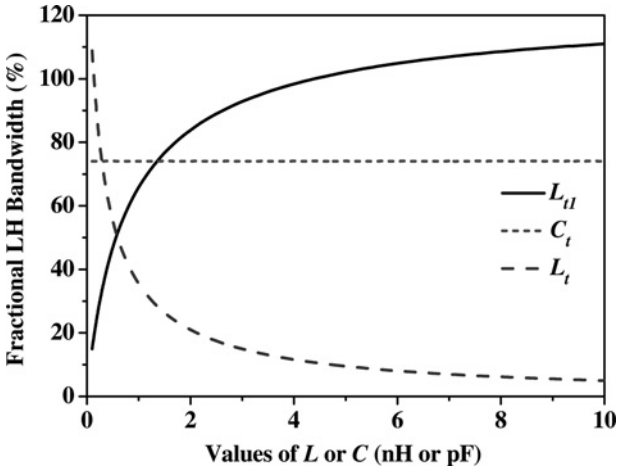

Figure 4 *Fractional LH bandwidth versus L_{t1}, C_t, and L_t (circuit simulation result using Ansoft's Designer)*

independent of the capacitances values of C_t. Consequently, the bandwidth of the PLH TL can be easily adjusted by only inductive component since it is independent on capacitive component. On the other hand, to obtain a broad fractional LH bandwidth of the CRLH TL, the values of RH elements (C_R, L_R) should be smaller than those of the LH elements (C_L, L_L) [2, 3]. In reality, once the unit length of d is determined (or fixed), it is impossible that the values of RH elements (C_R, L_R) simultaneously decrease for the broad LH bandwidth of the CRLH TL, where $C_R = C'_R d$ and $L_R = L'_R d$. Since the product of C'_R (F/m) and L'_R (H/m) is equal to $1/v_p^2$, where v_p is the phase velocity of a host TL without LH components. For example, if the width of host TL is wide for lager C'_R, the value of L'_R becomes small and vice versa. Therefore the proposed PLH TL has more flexibility to design the broad fractional LH bandwidth than the CRLH TL. Using the parameter study, the PLH TL with wide fractional LH bandwidth will be implemented in the next section.

3 Simulation and experiment

3.1 Fabrication

Figs. 5*a* and *b* show the top and bottom views of the fabricated two-stage PLH TL with a WBIDC. The input and output ports are fabricated using a 50 Ω coaxial connector. The width of the signal line is set to be 0.6 mm, corresponding to a 50 Ω line. The width and length of the feed line are optimised as 1.9 and 10.8 mm for impedance matching at 2.5 GHz, respectively. To have a broad PLH bandwidth and eliminate spurious resonances of an IDC, the proposed structure has a DGS with WBIDC. Through the parameter study using the equivalent circuit, the proposed structure is newly optimised to have a wide LH bandwidth. Figs. 5*c* and *d* show the top and bottom views of the optimised two-stage PLH TL with wide LH bandwidth. To increase the inductance values of L_{t1}, the signal line is replaced with a meander line. The width of connecting part to the feed line is

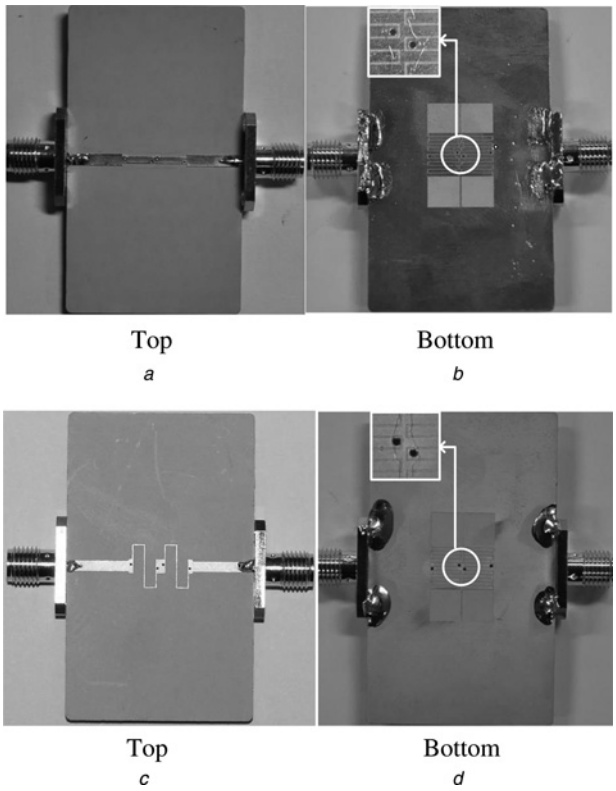

Figure 5 *Fabricated two-stage PLH TL*

a and *b* PLH with the WBIDC
c and *d* Optimised PLH TL with wide LH bandwidth
(Rogers RO3010 substrate: $h = .64$ mm, $\varepsilon_r = 10.2$)

broader to obtain lower inductance value of L_t. Thus, the width of the meander line and the connected part are set to be 0.2 and 2.3 mm, respectively.

3.2 S-parameters

Fig. 6 shows the measured *S*-parameters for two-stage PLH TLs. The PLH TL with the IDC has the first and second spurious mode at 2.41 and 3.61 GHz, whereas the PLH TL with the WBIDC has the first spurious mode at 4.2 GHz as shown in Fig. 6. Consequently, the PLH TL with WBIDC has broad LH bandwidth and is not affected by the spurious modes in LH band. (Simulated *S*-parameter data of PLH TLs are omitted to prevent from confusion.) The fractional bandwidth of PLH TL with IDC is 67% (1.119–2.26 GHz) whereas that of PLH TL with WBIDC is 83% (1.299–3.26 GHz). Also, the fractional bandwidth of the TL with wide bandwidth is 140% (0.624–3.51 GHz). Actually, the RH band does not exist, as it is expected, within BZ except for spurious mode by the IDC.

3.3 Dispersion curves

Fig. 7 shows the dispersion curves of the PLH TLs by theorem, full-wave simulation and measurement. The measurement results are in excellent agreement with those

IET Microw. Antennas Propag., 2010, Vol. 4, Iss. 6, pp. 792–798
doi: 10.1049/iet-map.2009.0084

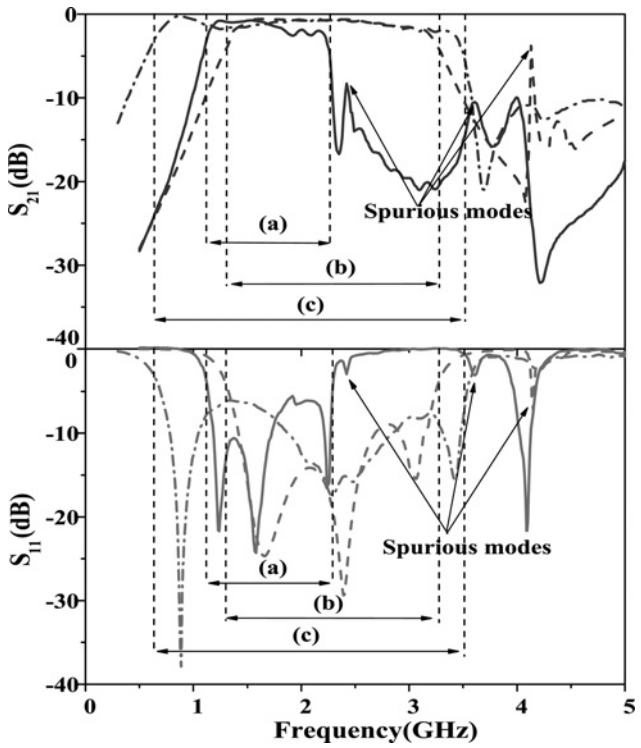

Figure 6 *S-parameters of PLH TLs*

a PLH TL with the IDC (solid line)
b PLH TL with the WBIDC (dash line)
c Optimised PLH TL with wide LH bandwidth (dash-dot line)

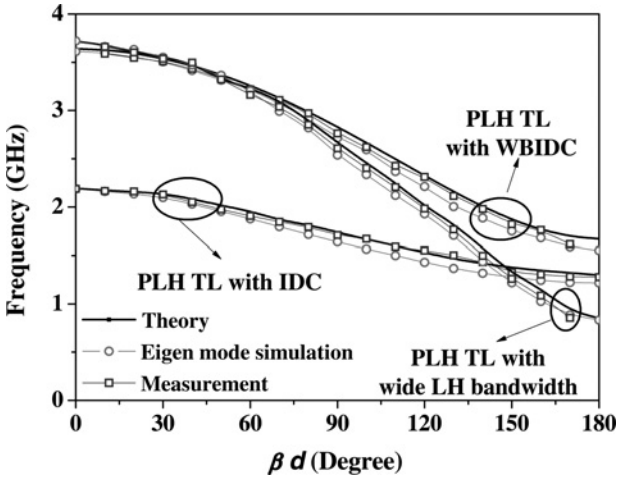

Figure 7 *Dispersion curves of PLH TLs (theoretical result using (4) and (5), eigenmode simulation result using Ansoft's HFSS)*

of simulation and theory. The dispersion characteristics of each PLH TL are compared in Fig. 7. The LH bands of each TL in Fig. 7 are in good agreement with those of *S*-parameters in Fig. 6. Also, these dispersion curves only have LH band without RH band in BZ. The fractional bandwidth of optimised PLH TL with wide LH bandwidth is boarder by ~70% compared to that of PLH TL with IDC. These results indicate that our proposed PLH TL could be successfully applied to the RF devices for broadband application and such as shifters, 180° hybrid ring, filters and baluns.

4 Conclusion

The PLH TL with a broad LH bandwidth, consisting of the DGS and WBIDC, is presented. The cross connection of vias to the ground makes the components of inductance and capacitance be effectively negative. These negative components get rid of the parasitic RH branch. Thus, the PLH TL can be designed. The properties of the PLH TL are analysed by the derived equivalent circuit, Bloch–Floquet theory, full-wave simulation and measurement. The results show good agreements. An optimised PLH TL with the wide LH fractional bandwidth of 140% is also demonstrated.

5 Acknowledgment

This work was supported by the IT R&D programme of KEIT (Korea Evaluation Institute of Industrial Technology). (2009-F-033-01, Study of technologies for improving the RF spectrum characteristics by using the meta-electromagnetic structure.)

6 References

[1] ENGHETA N., ZIOLKOWSKI R.W.: 'Metamaterials: physics and engineering explorations' (IEEE Press, 2006, 1st edn.)

[2] ELEFTHERIADES G.V., BALMAIN K.G.: 'Negative-refraction metamaterials: fundamental principles and applications' (IEEE Press, 2005, 1st edn.)

[3] CALOZ C., ITOH T.: 'Electromagnetic metamaterials: transmission line theory and microwave applications' (John Wiley, New Jersey, 2006, 1st edn.)

[4] GIL M., BONACHE J., SELGA J., GARCIA-GARCIA J., MARTIN F.: 'Broadband resonant-type metamaterial transmission lines', *IEEE Microw. Wirel. Compon. Lett*, 2007, **17**, (2), pp. 97–99

[5] ANTONIADES M.A., ELEFTHERIADES G.V.: 'Compact, linear, lead/lag metamaterial phase shfters for broadband applications', *IEEE Antennas Wirel. Propag. Lett.*, 2003, **2**, (7), pp. 103–106

[6] CALOZ C., ITOH T.: 'Transmission line approach of left-handed (LH) structures and microstrip realization of a low-loss broadband LH filter', *IEEE Trans. Antennas Progag.*, 2004, **52**, (5), pp. 1159–1166

[7] BRILLOUIN L.: 'Wave propagation in periodic structure: electric filters and crystal lattices' (Dover Inc., New York, 1946)

[8] CASARES-MIRANDA F.P., MARQUEZ-SEGURA E., OTERO P., CAMACHO-PENALOSA C.: 'Wire bonded interdigital capacitor', *IEEE Microw. Wirel. Compon. Lett.*, 2005, **15**, (10), pp. 700–702

[9] CASARES-MIRANDA F.P., MARQUEZ-SEGURA E., OTERO P., CAMACHO-PENALOSA C.: 'Composite right/left-handed transmission line with wire bonded interdigital capacitor', *IEEE Microw. Wirel. Compon. Lett.*, 2006, **16**, (11), pp. 624–626

[10] AHN D., PARK J.S., KIM J., QIAN Y., ITOH T.: 'A design of the low-pass filter using the novel microstrip defected ground structure', *IEEE Trans. Microw. Theory Tech.*, 2001, **49**, (9), pp. 83–93

[11] SCOTT R.E., ESSIGMAN M.W.: 'Linear circuits, part 1, time-domain analysis' (Addison Wesley, Tokyo, 1964, 1st edn.)

[12] STAELIN D.H., MORGENTHALER A.W., KONG J.A.: 'Electromagnetic waves' (Prentice-Hall, Inc., New Jersey, 1994, 1st edn.)

[13] POZAR D.M.: 'Microwave engineering' (John Wiley, Inc,, 1998, 2nd edn.)

doi: 10.1049/iet-map.2009.0084